SUPPLEMENTARY MATERIAL FOR
DYNAMICS AND FUNCTION OF COMPACT NUCLEOSOME ARRAYS

Michael G. Poirier[1,2], Eugene Oh[1], Hannah S. Tims[1], and Jonathan Widom[1]

[2]Department of Biochemistry, Molecular Biology and Cell Biology, Northwestern University, Evanston, IL 60208-3500.[2]Present address: Department of Physics, The Ohio State University, Columbus, OH 43210

Correspondence should be addressed to: mpoirier@mps.ohio-state.edu or j-widom@northwestern.edu.

SUPPLEMENTARY TEXT

Kinetic analysis

The stopped-flow FRET experiments (**Fig. 4d,f,g**) exhibit biphasic compaction kinetics, requiring a minimum of three conformational states. We designate the initial state of the nucleosome arrays, which are extended (since we start the experiment in the absence of Mg^{2+}), as S_4 (**Fig. 5**). The instantaneous increase in FRET upon Mg^{2+} addition implies an increase in compactness occurring within the mixing deadtime, ~1 millisecond (< 1msec). We designate the state achieved at this point as S_3, and conclude that the rate of $S_4 \rightarrow S_3$ (k_{43}) must be faster than 10^3 sec^{-1} (time constant shorter than 1 msec). The reverse rate ($S_3 \rightarrow S_4$, k_{34}) must be comparable to or slower than this forward rate, otherwise there would be negligible net compaction. The slower phase of the stopped-flow FRET data implies a second compaction, with comparable amplitude (change in FRET) to the first step, suggesting a comparable further increase in compactness. We designate the state so-formed as S_2. The time constant of this second step is ~2 sec, which, if the relaxation were dominated by the forward step (as will shortly be explained to be the case), implies a forward rate of ($S_3 \rightarrow S_2$, k_{32}) of ~0.5 sec^{-1}. Since the system is near-maximally compact in these conditions (**Fig. 1f**), it follows that the $S_3 \leftrightarrow S_2$ equilibrium must be largely shifted to S_2, implying that the reverse rate ($S_2 \rightarrow S_3$, k_{23}) is significantly slower than the forward (i.e., $k_{23} < 0.5$ sec^{-1}), and justifying the assignment of the observed relaxation rate to the forward rate, k_{32}.

Even after the system reaches steady state, however, FRET-FCS analysis (**Fig. 4a,c**) reveals that there exists a rapid interconversion between two states, with a relaxation time of ~10^{-5} sec, much faster than the rates for $S_3 \leftrightarrow S_2$, therefore requiring at least one additional compact state (S_1) connected reversibly to S_2. Moreover, the turnover time (1×10^{-5} sec) in this analysis equates to the reciprocal of the sum of the individual forward and reverse rate constants, $k_{21}+k_{12}$ (refs.[1-5]).

Two somewhat-different scenarios are consistent with these data. One possibility is that these two interconverting compact states differ only slightly in FRET (and thus, relatively little in compactness as well). In that case each of the two states

would need to have substantial occupancy, otherwise there would be no detectable FCS signal at all. This in turn implies that k_{21} would need to approximately equal k_{12} (since the equilibrium between these states is the ratio of the rate constants and is of order 1 in this scenario); and if $k_{21} \approx k_{12}$, yet $k_{21}+k_{12} = 1\text{x}10^5$ sec^{-1}, it follows that $k_{21} \approx k_{12} \approx 5\text{x}10^4$ sec^{-1}. An alternative possibility is that state S_1 has significantly greater FRET (and compactness) even than does S_2. In this case, the low amplitude of the FRET ratio function implies that the $S_1 \leftrightarrow S_2$ equilibrium must be largely shifted to S_2. This in turn implies that $k_{12} >> k_{21}$; and since $k_{21}+k_{12} = 1\text{x}10^5$ sec^{-1}, it follows that $k_{12} \approx 1\text{x}10^5$ sec^{-1}; and k_{21} is significantly slower, with a lower bound that boils down to a statement about the detectability of a large FRET change in a small fraction of the population. We can estimate a lower bound on the rate k_{21} by supposing that the FRET change from $S_2 \rightarrow S_1$ were as large as from 0 to 1 (which is necessarily an overestimate, given the FRET changes observed between earlier states S_2, S_3, and S_4 as well). Then the observed 0 lag time donor autocorrelation ratio of 1.04 would equate to an equilibrium constant of 1/0.04 = 25 (ref. [5]), which, together with the conclusion (in this alternative) that $k_{12} \approx 1\text{x}10^5$ sec^{-1}, implies that $k_{21} \approx 4\text{x}10^3$ sec^{-1}. And if the FRET values are less skewed (more similar) between these two states, the rate constants correspondingly must become closer, returning finally to the opposite limit discussed above, where the FRET values are nearly identical, and the rates approach equivalence. Thus from the FRET-FCS analysis we conclude that the forward rate ($S_2 \rightarrow S_1$, k_{21}) must fall in the range $4\text{x}10^3$ sec^{-1} to $5\text{x}10^4$ sec^{-1}; and the reverse rate ($S_1 \rightarrow S_2$, k_{12}) must fall in the range $5\text{x}10^4$ sec^{-1} to $1\text{x}10^5$ sec^{-1}.

Finally, we emphasize kinetic analyses can only *disprove* mechanisms. There necessarily exist more complex mechanisms (having more states), which are also capable of explaining the data presented here. The mechanism that we present represents the simplest possible mechanism that is compatible with the existing data. As discussed here, this simplest possible mechanism requires 4 states arranged as illustrated (**Fig. 5**).

SUPPLEMENTARY METHODS

Preparation of labeled DNAs.

Site exposure-sensitive mononucleosome DNA constructs.

The mononucleosome DNA template mp32 was PCR amplified with labeled primers: CATAAGGAGGGCAGTGAGCTGT(Cy3)AGAATCCCGGTGCCGAGGCCG CTCAATTGGTCGTAG and TCCTTATCCCCCCAGTGTCACAGGATGTATATATCTGACACGTGC CTGGAGACTAGGGAGTAATCCCCTTGGCGGTTAAAACGCGGT(Cy5)GGACA. The analogous DNA template with the LexA site, mp31, was PCR amplified with labeled primers: CATAAGGAGGGCAGTGAGCTGT(Cy3)AGATACTGTA TGAGCATACAGTACAATTGGTCGTAGCAAGCTCTAG and TCCTTATCCCCCCAGTGTCACAGG ATGTATATATCTGACACGTGCCTGGAGACTAGGGAGTAATCCCCTTGGCGGTTAAAACGCGGT(Cy5) GGACA. These DNA molecules were phenol-chloroform, chloroform and ether extracted and then purified by PAGE.

Compaction-sensitive nucleosome trimer array DNA constructs

Each individual 601 site within the trimer was synthesized by PCR. Their locations are designated 601-A, 601-B and 601-C, left to right. DNA constructs mp33, mp34, and mp37 were designed to measure array compaction, and the constructs, while mp35 and mp36 were designed as a control for aggregation. The 601-A DNA segment was PCR amplified by ATCGAAGACAGTACTGGCCGCCCTGGAGAATCCCGGTGCC and TCCTTATCCCCCCAGTGTC ACAGGATGTATATATCTGACACGTGCCTGGAGACT(Cy3, Alexa 568 or no label)AGGGAG. The trinucleosome 601-B DNA segment (for mp 34–37) was PCR amplified with DNA primers: CATAAGGAGGACACTGGGACATGCATCGGCTGGAGAATCCCGGTGCCGA and GTAGCGTCAA CTCACTGCCCTATGCATTATACAGGATGTATATATCTGACACGTGCCTG. The LexA site-containing trinucleosome 601-B (designated 601-B-L, for mp33) was PCR amplified with DNA primers: CATAAGGAGGACACTGGGACATGCATCGGCTGGAGATACTGTATGAGCATACAGTACAATTGGTCG and GTAGCGTCAACTCACTGCCCTATGCATTATACAGGATGTATATATCTGACACGTGC

CTG. The trinucleosome 601-C DNA segment was PCR amplified with DNA primers: CATAAGGAGGGCAGTGAGCTGGAGAATCCCGGTGCCGAGGCCGCTCAATTGGT(Cy5, Alexa 647, or no label)CGTAGC and ATCGAAGACAGAGTACTTACATGCACAGGATGTATATATCTGACACGTGCC. Each DNA segment was digested with TspRI and then sequentially extracted with 50% phenol/50% chloroform, 100% chloroform and ether. The ether was removed by spinning in a speedvac for 30 minutes. The DNA was then concentrated with a centricon 50 (Millipore). The three DNA segments 601-A, -B and -C were combined at equimolar ratio, then ligated with T4 ligase. The ligation was sequentially extracted with 50% phenol/50% chloroform, 100% chloroform and then ether. The DNA was again concentrated with a centricon 50. Typically, about 50% of the DNA converted into a 601 trimer. This was purified by PAGE, cloned into pDrive (Qiagen), and sequenced to confirm its identity.

Site exposure-sensitive nucleosome trimer array DNA constructs

Each 601 site in the trimer was separately PCR amplified. Again each 601 DNA segment is labeled as 601-A, 601-B (for DNA mp32) (or 601-B-L, for LexA site-containing, mp31) and 601-C. 601-A was synthesized by PCR amplification with DNA oligos: ATCGAAGACAGTACTGGCCGCCCTGGAGAATCCCGGTGCC and TCCTTATCCCCCCAGTGTCACAGGATGTATATATCTGACACGTGCCTGGAGACTAGGGAG. 601-B was synthesized by PCR amplification with DNA oligos: CATAAGGAGGGCAGTGAGCTGT(Cy3)AGAATCCCGGTGCCGAGGCCGCTCAATTGGTCGTAG and TCCTTATCCCCCCAGTGTCACAGGATGTATATATCTGACACGTGCCTGGAGACTAGGGAGTAATCCC CTTGGCGGTTAAAACGCGGT(Cy5)GGACA. This oligo contained a large fraction of shorter length products. Therefore it was purified by PAGE under denaturing conditions before the PCR amplification. 601-B-L was synthesized by PCR amplification with DNA oligos: CATAAGGAGGGCAGTGAGCTGT(CY3)AGATACTGTATGAGCATACAGTACAATTGGTCGTAGCAAGC TCTAG and TCCTTATCCCCCCAGTGTCACAGGATGTATATATCTGACACGTGCCTGGAGACTAGGGAGTAATCCC CTTGGCGGTTAAAACGCGGT(Cy5)GGACA. 601-C was synthesized by PCR amplification with DNA oligos: CATAAGGAGGACACTGGGACGAGGTGCGGCTGGAGAATCCCGGTGCCGA and GGCACGTGTCAGATATATACATCCTGTGCATGTAAGTACTCTGTCTTCGAT. The 601 trimer was

made as described above where each PCR product was digested with TspRI, ligated and then purified by PAGE, cloned, and sequenced.

REFERENCES

1. Bonnet, G., Krichevsky, O. & Libchaber, A. Kinetics of conformational fluctuations in DNA hairpin-loops. *Proc Natl Acad Sci USA* **95**, 8602-6 (1998).
2. Krichevsky, O. & Bonnet, G. Fluorescence correlation spectroscopy: the technique and its applications. *Reports on Progress in Physics* (2002).
3. Hess, S.T., Huang, S., Heikal, A.A. & Webb, W. Biological and chemical applications of fluorescence correlation spectroscopy: a review. *Biochemistry* **41**, 697-705 (2002).
4. Elson, E.L. & Webb, W.W. Concentration correlation spectroscopy: a new biophysical probe based on occupation number fluctuations. *Annu Rev Biophys Bioeng* **4**, 311-34 (1975).
5. Li, G., Levitus, M., Bustamante, C. & Widom, J. Rapid spontaneous accessibility of nucleosomal DNA. *Nat Struct Mol Biol* **12**, 46-53 (2005).

SUPPLEMENTARY FIGURE 1

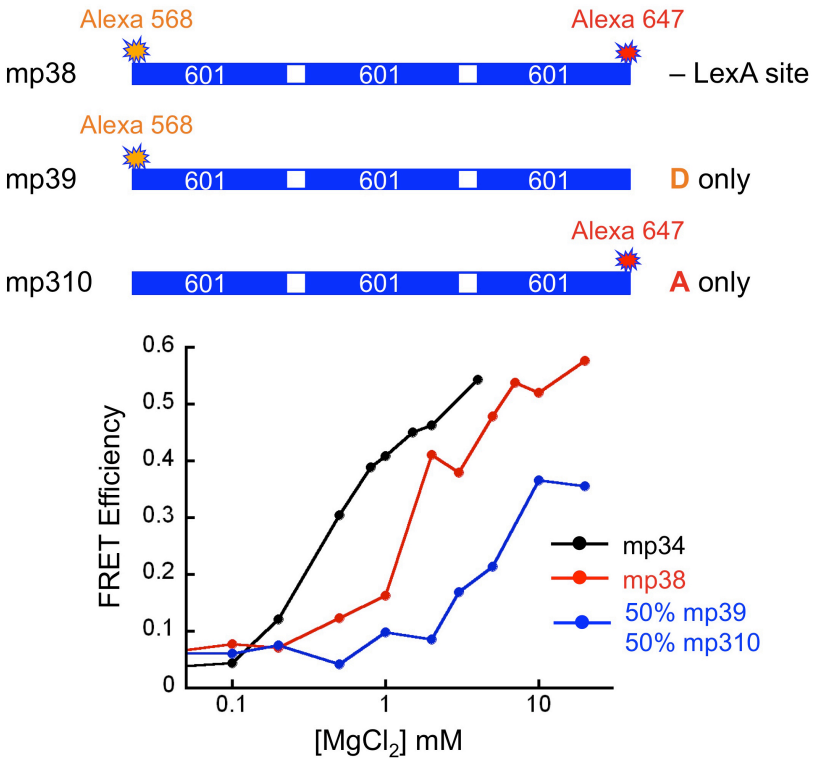

Supplementary Figure 1 Negative control FRET experiment. The donor and acceptor dyes in construct DNA mp38 do not neighbor closely in space in the compact structure as imaged by X-ray crystallography, and therefore may reveal Mg^{2+}-dependent aggregation but should not exhibit a high FRET signal from Mg^{2+}-dependent compaction in the range 0–1 mM Mg^{2+}. Consistent with this expectation, compared to the compaction sensitive FRET system (DNA mp34), FRET analysis of trinucleosome arrays constructed with DNA mp38 do not exhibit high FRET in 1 mM Mg^{2+}, but do reveal Mg^{2+}-dependent aggregation which occurs predominantly at higher Mg^{2+} concentration, as can be seen also in the mixture of the corresponding singly-labeled trinucleosome arrays (DNAs mp39, mp310).

SUPPLEMENTARY FIGURE 2

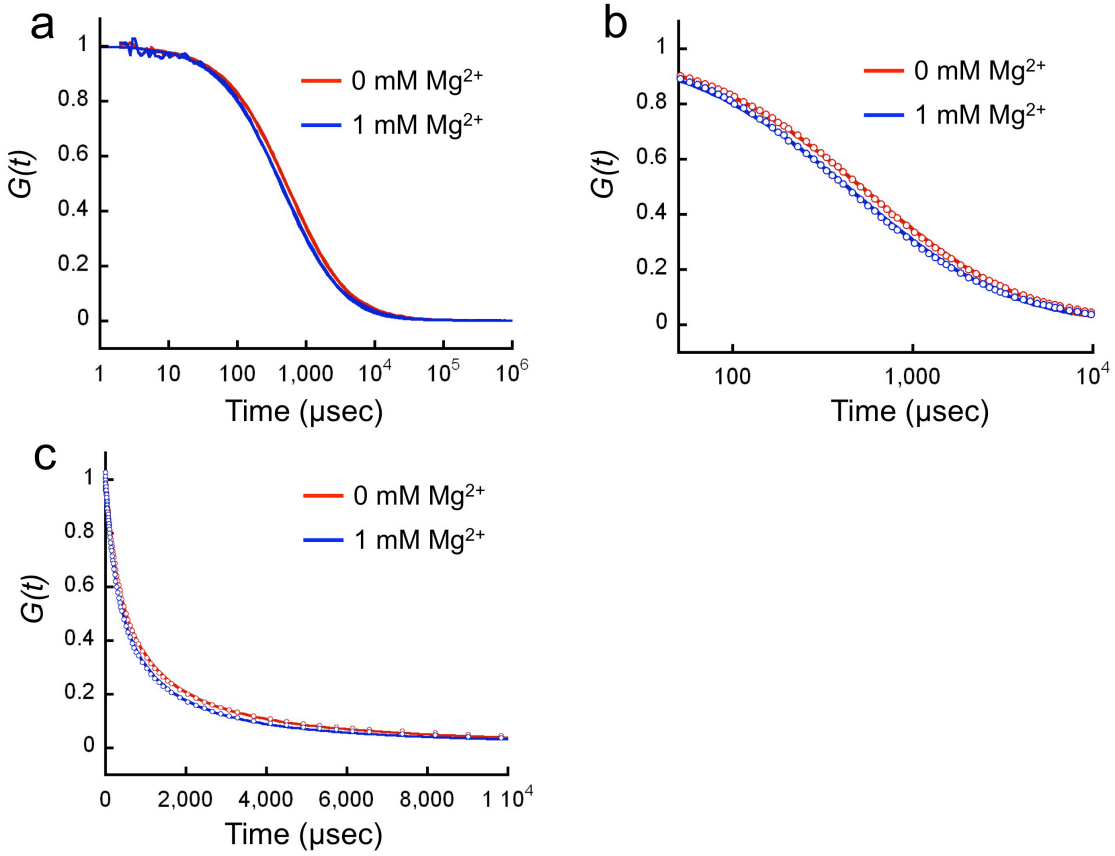

Supplementary Figure 2 Diffusion coefficients of trimer nucleosome arrays. (**a**) Normalized donor fluorescence autocorrelation of nucleosome arrays with DNA mp35 in 0 (red) and 1 mM (blue) Mg^{2+}. With addition of Mg^{2+}, the curve shifts to lower lag times, implying faster translational diffusion, and thus greater compactness. In independent experiments, the translational diffusion coefficient decreased by 17 ± 2% (mean and standard deviation, n=3) in the presence of 1 mM Mg^{2+}. Aggregation would imply larger sizes instead, which would decrease the diffusion coefficient, shifting the curve to larger lag times – contrary to observation. (**b**) Expanded scale plot of the data in (a). (**c**) Plot of the data in (a) on a linear scale.

SUPPLEMENTARY FIGURE 3

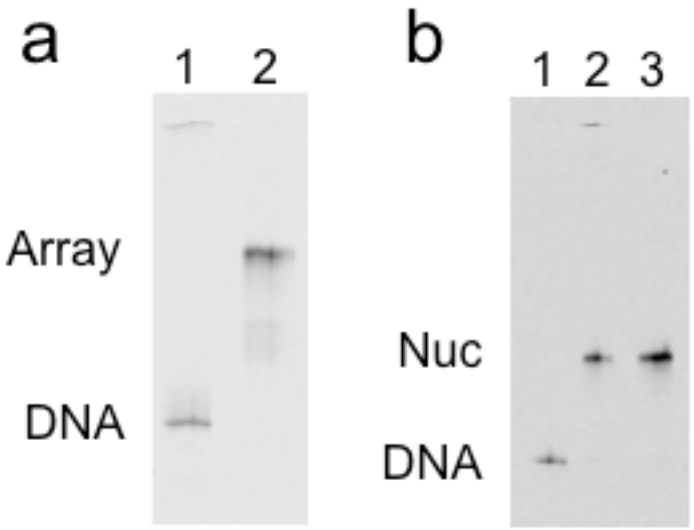

Supplementary Figure 3 Reconstitution and purification of site exposure sensitive trinucleosome arrays and mononucleosomes. (**a**) Native polyacrylamide gel analysis of naked mp32 DNA (lane 1) and reconstituted nucleosome arrays after sucrose gradient purification (lane 2) showing fluorescence image of Cy5 dye. (**b**) Native polyacrylamide gel analysis of naked mp12 DNA (lane 1), reconstituted mononucleosomes (lane 2), and after sucrose gradient purification (lane 3) showing fluorescence image of Cy5 dye.